Am J Physiol Lung Cell Mol Physiol 293: L923–L932, 2007.
First published July 27, 2007; doi:10.1152/ajplung.00221.2007.

TRPV4 initiates the acute calcium-dependent permeability increase during ventilator-induced lung injury in isolated mouse lungs

Kazutoshi Hamanaka,[1,4] Ming-Yuan Jian,[1,4] David S. Weber,[1] Diego F. Alvarez,[1,4] Mary I. Townsley,[1,4] Abu B. Al-Mehdi,[2,4] Judy A. King,[2,3,4] Wolfgang Liedtke,[5] and James C. Parker[1,4]

Departments of [1]Physiology, [2]Pharmacology, and [3]Pathology and [4]Center for Lung Biology, University of South Alabama, Mobile, Alabama; and [5]Department of Medicine, Neurology, and Neurobiology, Duke University, Durham, North Carolina

Submitted 4 June 2007; accepted in final form 21 July 2007

Hamanaka K, Jian M-Y, Weber DS, Alvarez DF, Townsley MI, Al-Mehdi AB, King JA, Liedtke W, Parker JC. TRPV4 initiates the acute calcium-dependent permeability increase during ventilator-induced lung injury in isolated mouse lungs. *Am J Physiol Lung Cell Mol Physiol* 293: L923–L932, 2007. First published July 27, 2007; doi:10.1152/ajplung.00221.2007.—We have previously implicated calcium entry through stretch-activated cation channels in initiating the acute pulmonary vascular permeability increase in response to high peak inflation pressure (PIP) ventilation. However, the molecular identity of the channel is not known. We hypothesized that the transient receptor potential vanilloid-4 (TRPV4) channel may initiate this acute permeability increase because endothelial calcium entry through TRPV4 channels occurs in response to hypotonic mechanical stress, heat, and *P*-450 epoxygenase metabolites of arachidonic acid. Therefore, permeability was assessed by measuring the filtration coefficient (K_f) in isolated perfused lungs of C57BL/6 mice after 30-min ventilation periods of 9, 25, and 35 cmH_2O PIP at both 35°C and 40°C. Ventilation with 35 cmH_2O PIP increased K_f by 2.2-fold at 35°C and 3.3-fold at 40°C compared with baseline, but K_f increased significantly with time at 40°C with 9 cmH_2O PIP. Pretreatment with inhibitors of TRPV4 (ruthenium red), arachidonic acid production (methanandamide), or *P*-450 epoxygenases (miconazole) prevented the increases in K_f. In TRPV4$^{-/-}$ knockout mice, the high PIP ventilation protocol did not increase K_f at either temperature. We have also found that lung distention caused Ca^{2+} entry in isolated mouse lungs, as measured by ratiometric fluorescence microscopy, which was absent in TRPV4$^{-/-}$ and ruthenium red-treated lungs. Alveolar and perivascular edema was significantly reduced in TRPV4$^{-/-}$ lungs. We conclude that rapid calcium entry through TRPV4 channels is a major determinant of the acute vascular permeability increase in lungs following high PIP ventilation.

pulmonary edema; *P*-450 epoxygenases; stretch-activated cation channel; vascular permeability; Ca^{2+} channels; epoxyeicosatrienoic acids; temperature

ACUTE LUNG INJURY (ALI) and the acute respiratory distress syndrome (ARDS) are life-threatening conditions caused by a variety of pathologic processes and affect over 200,000 patients in the United States each year (41). Although positive pressure mechanical ventilation is a life-saving intervention in the setting of ARDS and ALI, clinical trials have demonstrated that mechanical ventilation with excessive tidal volumes actually contributes to lung injury and increases mortality (6). Although clinicians and researchers have been interested in ventilator-induced lung injury (VILI) for decades, the molecular mechanisms driving this process remain incompletely understood (7, 8, 27, 48).

Many previous investigators have reported that high airway pressures and lung volumes can increase pulmonary endothelial and epithelial permeability (7, 8, 27). An altered ion channel activity occurs within seconds in response to mechanical stress, and an increase in intracellular Ca^{2+} concentration ($[Ca^{2+}]_i$) is a necessary component for the increased vascular permeability associated with numerous types of insult (4, 18, 19, 30). Parker et al. (28) proposed that stretch-activated cation channels might initiate the increase in permeability induced by mechanical ventilation through increases in $[Ca^{2+}]_i$, because gadolinium, which blocks stretch-activated nonselective cation channels, prevented the increases in vascular permeability induced by high airway pressure ventilation in isolated rat lungs. Although the molecular identity of these stretch-activated cation channels has not been established, recent evidence suggests that these mechanogated channels may belong to the transient receptor potential vanilloid (TRPV) family of channel proteins.

TRPV4 is a Ca^{2+}-permeable cation channel gated by a diverse range of stimuli. TRPV4 was initially identified as a channel activated by membrane stretch induced by osmotic stimuli (14). Further study demonstrated that TRPV4 is also activated by heat (11, 43), mechanical stimuli (23), the synthetic phorbol ester 4α-phorbol 12,13-didecanoate (4α-PDD) (3, 43), cytochrome *P*-450 epoxygenase-dependent formation of epoxyeicosatrienoic acids (EETs) from arachidonic acid (3, 44, 45), and bisandrographolide A (BAA), a compound from *Andrographis paniculata,* a plant used in traditional medicine in many regions of Asia (34). TRPV4 is expressed in a broad range of tissues, including lung, spleen, kidney, testis, fat, brain, cochlea, skin, smooth muscle, liver, and vascular endothelium (13, 22, 40).

In the present study, we tested the hypothesis that TRPV4 initiates the increase in endothelial permeability as measured by the filtration coefficient (K_f) in isolated mouse lungs in response to ventilation with high peak inflation pressures (PIP). The role of TRPV4 was investigated using a TRPV channel inhibitor and TRPV4 knockout mice as well as inhibitors of known arachidonic acid-derived gating compounds over a range of temperatures. We also tested whether alveolar distention caused a $[Ca^{2+}]_i$ increase in isolated mouse lungs in the presence or absence of TRPV4 activity using fluorescence microscopy.

Address for reprint requests and other correspondence: J. C. Parker, Dept. of Physiology, College of Medicine, MSB 3074, Univ. of South Alabama, 307 Univ. Blvd., Mobile, AL 36688 (e-mail: Jparker@usouthal.edu).

The costs of publication of this article were defrayed in part by the payment of page charges. The article must therefore be hereby marked "*advertisement*" in accordance with 18 U.S.C. Section 1734 solely to indicate this fact.

METHODS

All experimental protocols were approved by the Institutional Animal Care and Use Committee of the University of South Alabama College of Medicine. Anesthetized mice were euthanized by exsanguination at the time of heart and lung removal.

Isolated lung preparation. C57BL/6 male mice (Charles River Laboratory), weighing 19.6–32.0 g (24.1 ± 0.3 g), were anesthetized with an intraperitoneal injection of pentobarbital sodium (100 mg/kg). The trachea was cannulated, and the mice were ventilated with a gas mixture of 20% O_2-5% CO_2-75% N_2 by use of a Harvard rodent ventilator (model no. 683; Harvard, South Natick, MA). The tidal volume was adjusted to obtain a PIP of ~9 cmH_2O at a respiratory rate of 40 breaths/min, with a positive end-expiratory pressure (PEEP) of ~2.5 cmH_2O. The chest was opened, 100 IU of heparin sodium was injected into the right ventricle, and a suture was placed around the pulmonary artery with aorta. Cannulas (0.86 mm internal diameter, 1.27 mm outside diameter) were placed in the pulmonary artery and left atrium, and lung and heart were excised en bloc and suspended from a balance beam attached to a force transducer (model FT03 C; Grass, Quincy, MA). The initial 1–2 ml of perfusate, which contained residual blood cells and plasma, were discarded and not recirculated. All lungs were perfused with 1% bovine serum albumin-3% clinical grade dextran in Earle's buffer salt solution by using a roller pump (Minipuls2; Gilson, Middleton, WI) at a constant flow rate of 0.75 ml/min in a recirculating system that had a system volume of 10 ml. The venous outflow was collected in a reservoir, the height of which could be adjusted to increase venous pressure. Pulmonary arterial pressure (Ppa) and pulmonary venous pressure (Ppv) were zeroed at the midlung level, and airway pressure (Paw) was measured by using Cobe pressure transducer (Lakewood, CO); pressures and lung weight were continuously recorded on a Grass model 7D polygraph (20).

Filtration coefficient. After 30 min, an isogravimetric state was attained; Ppv was increased by 6 cmH_2O for 20 min, and the change in capillary pressure (Ppc) was determined by double occlusion before and after the Ppv increase. K_f (in $ml \cdot min^{-1} \cdot cmH_2O^{-1} \cdot 100\ g^{-1}$) was calculated as the rate of lung weight gain between 18 and 20 min divided by the change in Ppc. All K_f values were normalized to 100 g predicted lung weight (PLW) on the basis of the ratio of lung weight to body weight (BW) according to PLW = (0.00452 ± 0.0003) BW (26).

Experimental protocols. The lungs were ventilated with 9 cmH_2O PIP throughout the experiment (low PIP) or 25 and 35 cmH_2O (high PIP) with PEEP of ~2.5 cmH_2O at 40 breaths/min. Perfused buffer was preheated to target temperature at 30, 35, or 40°C before the experiments were started, and the lungs were also directly heated with a surrounding water flow container that was connected to the water bath. The lungs were randomly allocated to one of the following protocols: low PIP/30°C, high PIP/30°C, low PIP/35°C, high PIP/35°C, low PIP/40°C, high PIP/40°C. The time course of airway and venous pressure increases in the high PIP group is shown in Fig. 1. K_f was measured at 30, 80, and 130 min. The target temperatures were obtained by direct measurement of the perfusate at the end of the experiments. We also measured the temperature during the experiment by using a type K thermometer (Extech Instruments, Wartham, MA) probe inserted into the mouse right ventricle.

Lung wet-to-dry weight ratios. After the measurement of final K_f, the lung was harvested, wet weight was determined, and samples were desiccated at 80°C for 1 wk before the dry weight was determined; the ratio of wet to dry weight was calculated as the wet-to-dry lung weight ratio (W/D ratio).

Inhibition of TRPV4 activation. K_f and W/D ratio measurement were performed in low PIP/35°C, high PIP/35°C, low PIP/40°C, and high PIP/40°C protocols, with the same time course as described above. The following inhibiting drugs were added as a bolus to the venous reservoir of the perfusion system 20 min before the first K_f measurement: 20 μM ruthenium red, a TRPV channel inhibitor; 10 μM methanandamide, an arachidonic acid antagonist; and 10 μM miconazole, a *P*-450 epoxygenase inhibitor.

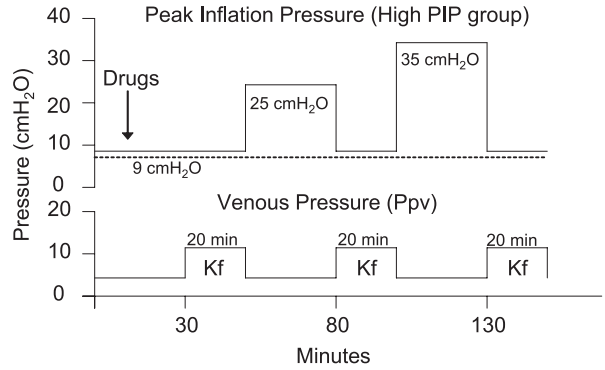

Fig. 1. Time course of peak inflation pressures (PIP) in high PIP (solid line) and low PIP (dashed line) ventilation protocols and venous pressures used in both protocols. K_f, filtration coefficient; Ppv, pulmonary venous pressure.

Ratiometric fluorescence microscopy. We used an intravital microscopy technique to observe and image endothelial cells in the isolated mouse lung (36). Wild-type ($TRPV4^{+/+}$) and TRPV4 knockout ($TRPV4^{-/-}$) mice were ventilated with a Minivent mouse ventilator (Hugo Sachs Elektronik-Harvard Apparatus); lung and heart were isolated and perfused with Earle's buffer containing 1% albumin and 3% dextran by use of a roller pump (Reglo Digital, Compact cassette pump, Ismatec). Lungs were loaded with fluo-4 (3 μM) and fura red (5 μM) for 25 min and subsequently perfused with dye-free perfusate for 20 min to wash out intravascular dye to reduce background fluorescence. The perfusate was discarded and not recirculated during this period. Then the lung was placed onto the coverslip window at the bottom of the chamber with the posterior surface of the lung gently touching the coverslip. The chamber with an isolated mouse lung was placed on the stage of an epifluorescence microscope fitted with a ×20 objective. Excitation of the lung surface was accomplished with a 120-W metal halide lamp (E-cite 120; Exfo Photonics Solutions, Mississauga, ON, Canada), and appropriate filter settings as follows: for fluo-4, 494-nm excitation, 516-nm emission; for fura red, 472-nm excitation, 646-nm emission. An inverted Nikon TE-2000 fluorescence microscope, automated 10-position filter wheels for both excitation and emission (Sutter Instruments, Lambda 10-2), automated dichroic filter cube changer (Nikon), *xy*-axis automated stage (Prior Scientific,), *z*-axis motor (Prior), a high-resolution 12-bit C4742-95-12ERG IEEE 1394 digital CCD camera (Hamamatsu), and MetaMorph image acquisition, processing, and analysis software were used for high-resolution digital imaging. A high-quality GFP filter set (Chroma Technology, Brattleboro, VT) was used. Images of fluo-4- and fura red-stained vascular endothelial cells were sequentially acquired every 15 s, and inflation pressure was increased to 15, 25, and 35 cmH_2O over 1-min periods. Ventilation was suspended during the period of data acquisition. Ca^{2+} intensity was measured with MetaMorph imaging software (Universal Imaging, West Chester, PA), and fluo-4/fura red fluorescence intensity ratio was calculated. Three groups were included in this experiment: $TRPV4^{+/+}$ mice, ruthenium red-treated $TRPV4^{+/+}$ mice, and $TRPV4^{-/-}$ mice; 20 μM ruthenium red was added to the perfusate after loading of fluorescence dyes.

Microscopic assessment of edema distribution. Light microscopy was used to evaluate edema distribution in glutaraldehyde-fixed lungs (2, 3) in high PIP/40°C and low PIP/30°C protocols, both wild-type and $TRPV4^{-/-}$ mice, after the experimental time course described in Fig. 1. Using 1-μm semithin sections, extra-alveolar vessel cuffing and alveolar flooding were evaluated. Cuff frequency and the edema cuff volume (V_c) fraction of total wall volume (V_c/V_w) were deter-

mined, the latter using a point-counting strategy. Point counting was used to determine the alveolar fluid volume (V_{af}) fraction in the alveolar space (V_{af}/V_{as}). Means for cuff frequency, cuff edema volume fractions, and alveolar fluid volume fractions were determined separately for each lung and overall descriptive statistics derived for each group.

Drugs. Methanandamide was obtained from Calbiochem. Fluo-4 AM and fura red AM were obtained from Invitrogen (Eugene, OR). All other drugs were obtained from Sigma (St. Louis, MO). Ruthenium red was dissolved in H_2O and stored at room temperature. Methanandamide was dissolved in DMSO, aliquoted, and stored at −70°C. Miconazole was dissolved in DMSO and stored at room temperature. Fluo-4 AM and fura red were dissolved in DMSO before use.

TRPV4 tyrosine phosphorylation. Tyrosine phosphorylation of TRPV4 was measured in lung homogenate by immunoprecipitation using anti-tyrosine phosphate antibody on agarose beads followed by immunoblots using an anti-TRPV4 antibody. An immunoprecipitation with antibodies in the reverse order was also performed. After isolated lung experiments, the right lung was frozen in liquid nitrogen (20) and stored at −70°C until analysis. For protein extraction, tissue samples were minced and sonicated, cells were lysed in ice-cold buffer at 4°C for 1 h, pH 7.4 (in mM: 50 HEPES, 5 EDTA, 100 NaCl), 1% Triton X-100, protease inhibitors (10 μg/ml aprotinin, 1 mM phenylmethylsulfonyl fluoride, 10 μg/ml leupeptin), and phosphatase inhibitors (in mM: 50 sodium fluoride, 1 sodium orthovanadate, 10 sodium pyrophosphate, 0.001 microcystin). Solubilized proteins were isolated using centrifugation (27,000 *g* for 15 min), and protein concentrations of the supernatant were determined using the Bradford assay. For Western analysis, samples were boiled in 1× SDS buffer, separated using SDS-PAGE, and subsequently transferred to nitrocellulose membranes. Membranes were blocked at room temperature for 1 h in TBS containing 5% milk and 0.1% Tween 20. Following incubation with primary and secondary antibodies, proteins were detected by enhanced chemiluminescence. For immunoprecipitation, cell lysates were incubated with anti-TRPV4 antibodies, and the immunocomplexes were collected with either A or G Plus-agarose beads for 3 h at 4°C. Following a rinsing, samples were boiled in 1× SDS buffer before Western blotting procedures. Western blot analysis was then performed using an anti-phosphotyrosine antibody. Band intensity was quantified using Sigmagel software.

A goat anti-TRPV4 polyclonal antibody from Alomone was used for immunoprecipitation, and a polyclonal rabbit anti-phosphotyrosine antibody was obtained from Upstate Biotechnology (Lake Placid, NY). Protein A Plus-agarose, and protein G Plus-agarose were purchased from Santa Cruz Biotechnology (Santa Cruz, CA).

Statistical analysis. All values are expressed as means ± SE. A two-way analysis of variance (ANOVA) with repeated measures followed by a Student-Newman-Keuls post-test was used. Significant differences were determined where $P < 0.05$.

RESULTS

K_f and edema responses to temperature and airway pressure. To investigate the response to high PIP ventilation and temperature in isolated perfused mouse lungs, we measured K_f and W/D ratio at different perfusate temperatures and PIP. Mean perfusate temperatures entering the lung were 30.0 ± 0.05, 35.0 ± 0.06, and 39.7 ± 0.08°C for the 30, 35, and 40°C groups, respectively. However, mean perfusate temperatures exiting the lung at the left ventricle were 32.5 ± 0.1 and 36.4 ± 0.1°C in 35 and 40°C groups, respectively. The K_f was unchanged at 30 and 35°C during the low PIP ventilation protocols (Fig. 2*A*), but K_f increased significantly to 2.3-fold of baseline after 35 cmH_2O PIP ventilation at 35°C (Fig. 2*B*). In contrast, the K_f was significantly increased at 40°C in both the

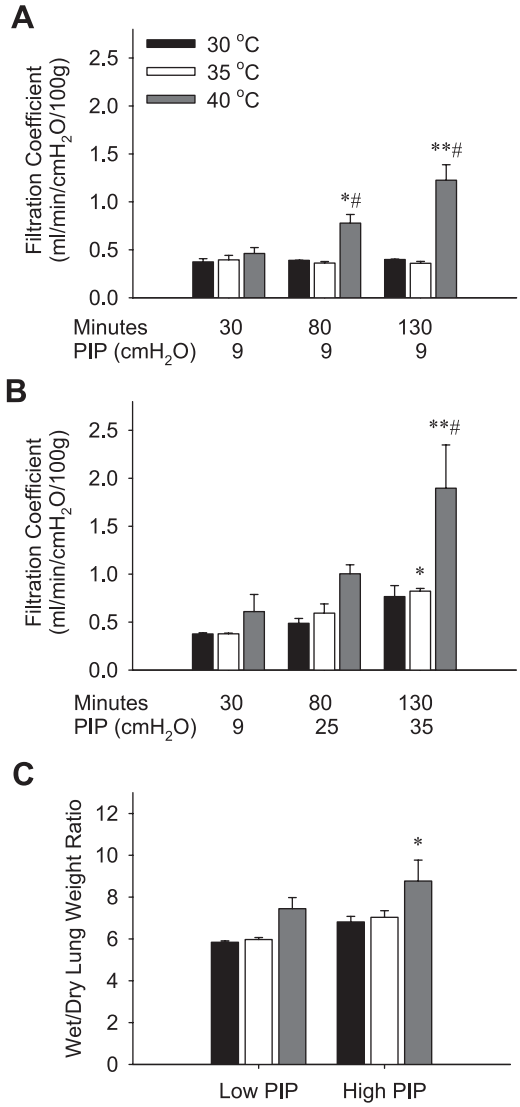

Fig. 2. K_f at 30, 35, and 40°C in low PIP (*A*) and high PIP (*B*) ventilation protocol groups. Wet-to-dry lung weight ratio of the same protocols (*C*). *$P <$ 0.05 vs. 30 min in same group. **$P < 0.05$ vs. 30 and 80 min in same group. #$P < 0.05$ vs. 30 and 35°C in same time.

low and high PIP ventilation protocols. In the low PIP group at 40°C, there was a trend toward an increase in mean baseline K_f, but K_f was significantly increased at 130 min by 3.4-fold compared with the 35°C baseline K_f (Fig. 2*A*). In the high PIP group ventilated at 40°C, mean baseline K_f tended to be increased compared with that at 35°C but was significantly increased by ventilation with 25 and 35 cmH_2O PIP, which increased K_f by 2.5- and 4.8-fold, respectively, compared with the baseline K_f at 35°C (Fig. 2*B*). The W/D ratios were indicative of the edema gained during the experiments. Since previous studies of unventilated lungs indicated a baseline W/D ratio of 4.3 ± 0.07 (49), the lungs gained weight even during low PIP ventilation because of filtration during the increased venous pressures used for K_f measurements. W/D ratio increases relative to unventilated lungs were 36, 39, and 78% after low PIP ventilation at 30, 35, and 40°C, respectively. Thus a portion of the lung edema sufficient to increase the W/D ratio ~40% from unventilated lungs could be attributed to the

perfusion protocol and filtration that occurred during the increased vascular pressure used for the K_f measurements, even without an increase in vascular permeability. In high PIP ventilated lungs, the mean W/D increases relative to unventilated lungs were 58, 63, and 95% for the respective temperatures. Although all mean W/D ratios were greater after high PIP than low PIP ventilation, only the high PIP/40°C and the low PIP/35°C groups were statistically different from each other (Fig. 2*C*). Since there were no significant differences between the 35 and 30°C groups, we chose target temperatures of 35 and 40°C for subsequent experiments.

VILI in TRPV4 null mice. To determine whether the K_f increases induced by high pressure ventilation and heating were initiated by TRPV4 channel activation, we repeated the protocols in TRPV4$^{-/-}$ knockout mice. The temperature- and pressure-induced increases in K_f observed in TRPV4$^{+/+}$ mice were significantly reduced in the TRPV4$^{-/-}$ mouse lungs in all pressure and temperature protocols (Fig. 3, *A–D*). The K_f in TRPV4$^{-/-}$ mouse lungs was essentially unchanged at 35°C after both low and high PIP ventilation and at 40°C during the low PIP protocol (Fig. 4, *A–C*). However, a 1.8-fold increase of K_f from baseline was observed at 40°C after 35 cmH_2O PIP ventilation that did not reach statistical significance. K_f in TRPV4$^{-/-}$ mouse lungs was significantly lower than that for TRPV4$^{+/+}$ mice after 25 and 35 cmH_2O PIP ventilation at both 35 and 40°C and after 80 and 130 min of low PIP ventilation in the 40°C group (Fig. 3*D*). W/D ratios also indicated significantly less lung edema formation in TRPV4$^{-/-}$ mice than TRPV4$^{+/+}$ mice (Fig. 3*E*).

Inhibitors of TRPV4 activation pathways. TRPV4 is activated by EETs generated through cytochrome *P*-450 epoxygenase metabolism from arachidonic acid (39). We investigated the effects of ruthenium red, methanandamide, and miconazole, which are inhibitors of TRPV4 or its activating pathways. Ruthenium red is an inhibitor of vanilloid TRP channels (TRPV1–6), miconazole is a nonselective inhibitor of cytochrome *P*-450, and methanandamide is a stable synthetic analog of the endocannabinoid anandamide and a nonselective inhibitor of anandamide metabolizing enzymes (45). These inhibitors all significantly reduced the K_f increases induced by high pressure ventilation and heat (Fig. 4, *A* and *B*). Furthermore, these inhibitors slightly reduced the increase in the lung W/D ratios induced by high airway pressures and heat (Fig. 4*E*).

Tyrosine phosphorylation of TRPV4. Since tyrosine phosphorylation of TRPV4 has been associated with activation of

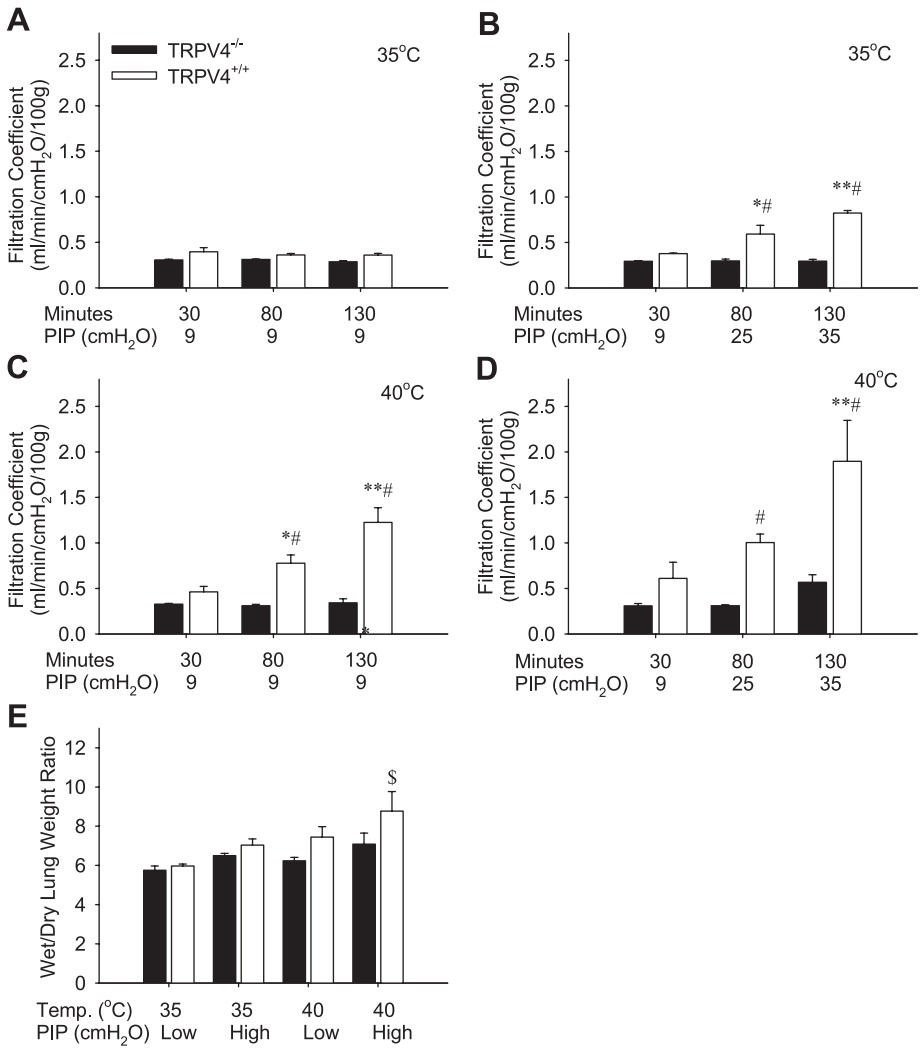

Fig. 3. K_f in transient receptor potential vanilloid-4 (TRPV4) wild-type (TRPV4$^{+/+}$) and knockout (TRPV4$^{-/-}$) mice in 35°C/low PIP (*A*), 35°C/high PIP (*B*), 40°C/low PIP (*C*), and 40°C/high PIP (*D*) protocols and wet-to-dry lung weight ratio in all protocols (*E*). *$P < 0.05$ vs. 30 min in same group. **$P < 0.05$ vs. 30 and 80 min in same group. #$P < 0.05$ vs. TRPV4$^{-/-}$ in same time. \$$P < 0.05$ vs. 35°C/low PIP in TRPV4$^{+/+}$.

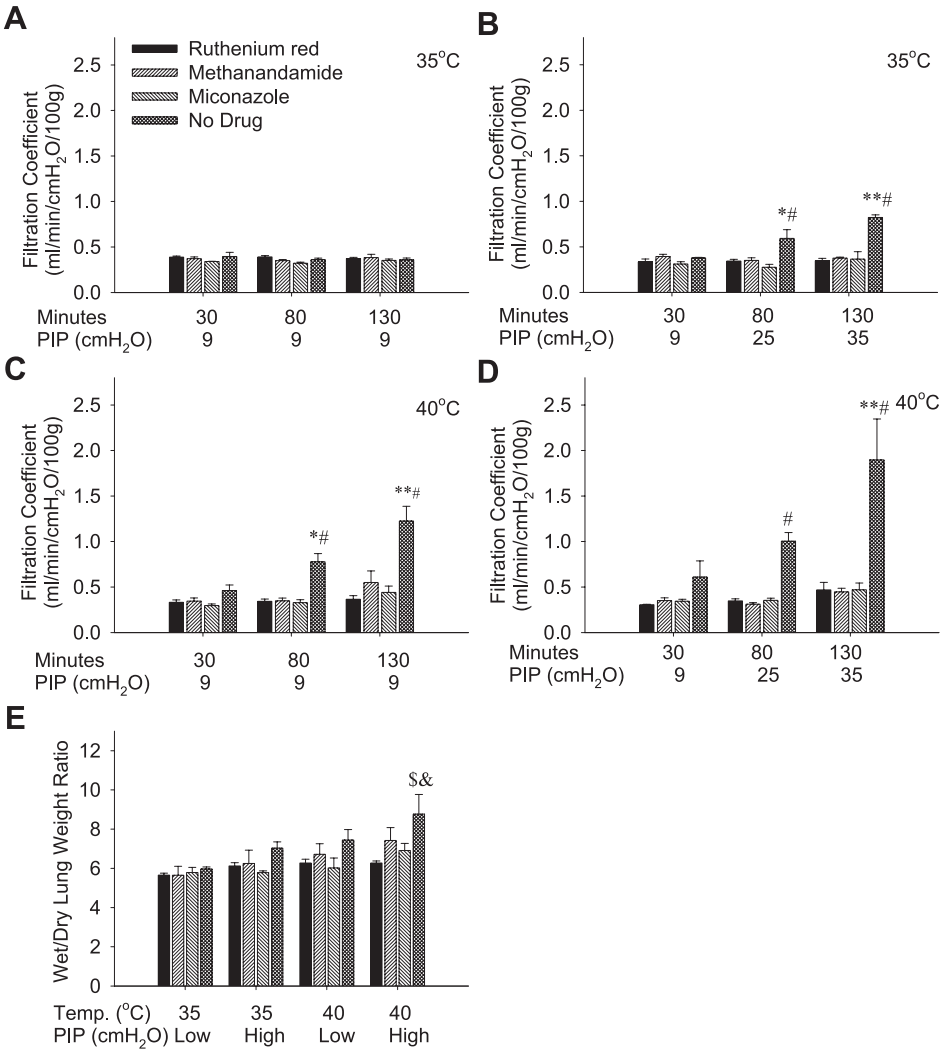

Fig. 4. Effect of TRPV4 inhibitors ruthenium red, methanandamide, and miconazole on K_f in 35°C/low PIP (*A*), 35°C/high PIP (*B*), 40°C/low PIP (*C*), and 40°C/high PIP (*D*) protocols. *$P <$ 0.05 vs. 30 min in same group. **$P < 0.05$ vs. 30 and 80 min in same group. #$P < 0.05$ vs. all other groups at same time. \$$P < 0.05$ vs. 35°C/low PIP and 35°C/high PIP. &$P < 0.05$ vs. ruthenium red and miconazole in 40°C/high PIP groups.

the channel (46), the tyrosine phosphorylation state of TRPV4 in lungs with no ventilation, low PIP ventilation at 35°C, and high PIP ventilation at 40°C was determined. Tyrosine-phosphorylated proteins were immunoprecipitated from lung tissue homogenates and membranes immunoblotted for TRPV4. An immunoprecipitation with antibodies in the reverse order was also performed with similar results (data not shown). Figure 5 shows the mean values for phosphorylated TRPV4 obtained in three separate lungs in each of the three groups. Tyrosine phosphorylation of TRPV4 was significantly increased in lungs after low PIP ventilation (2.3-fold) and high PIP ventilation (2.0-fold) compared with unventilated lungs, but there was no statistical difference between ventilation groups. An increased tyrosine phosphorylation of TRPV4 suggests activation of the channel by the mechanical stress of mechanical ventilation.

Ca^{2+} imaging by fluorescence microscopy. To evaluate the Ca^{2+} response of lung distention caused by high inflation pressures in isolated mouse lungs, we performed ratiometric Ca^{2+} imaging by the combined dye labeling with fluo-4 and fura red (Fig. 6). A ratiometric approach was used to correct for thinning of the cytoplasm of alveolar capillary endothelium during lung distention at high airway pressure. Fluorescence intensity of these dyes changes in opposite directions with increased $[Ca^{2+}]_i$. Fluo-4/fura red fluorescence intensity ratios showed a phased increase during inflation with 15, 25, and 35 cmH_2O of constant airway pressure in $TRPV4^{+/+}$ mice, with the ratios being 102.7, 108.1, and 112.8% for pressures of 15, 25, and 35 cmH_2O, respectively. In contrast, the ratios were 100.5, 98.8, and 97.0% in ruthenium red-treated mice and 100.0, 99.3, and 97.7% in $TRPV4^{-/-}$ mice for respective pressures of 15, 25, and 35 cmH_2O. The decreased ratio with time in $TRPV4^{-/-}$ and ruthenium red-treated mouse lungs may be caused by a reduction of Ca^{2+} signal due to the thinning of the interstitial tissue or by more rapid photobleaching of fluo-4 compared with fura red.

Assessment of light microscopy and transmission electron microscopy. Results of the morphometric analysis from light microscopy are shown in Fig. 7. Representative micrographs of lungs from the low PIP/30°C group (Fig. 7, *A* and *C*) or high PIP/40°C group (Fig. 7, *B* and *D*) in $TRPV4^{-/-}$ (Fig. 7, *A* and *B*) or wild-type mice (Fig. 7, *C* and *D*) are shown. Mean values for Vc/Vw (Fig. 7*E*) and Vaf/Vas (Fig. 7*F*) obtained using a point-counting strategy are also shown. Detectable edema cuff volumes but minimal alveolar flooding were obtained in both phenotypes after low PIP ventilation at 30°C because of edema formed during the three K_f measurements. Alveolar fluid was

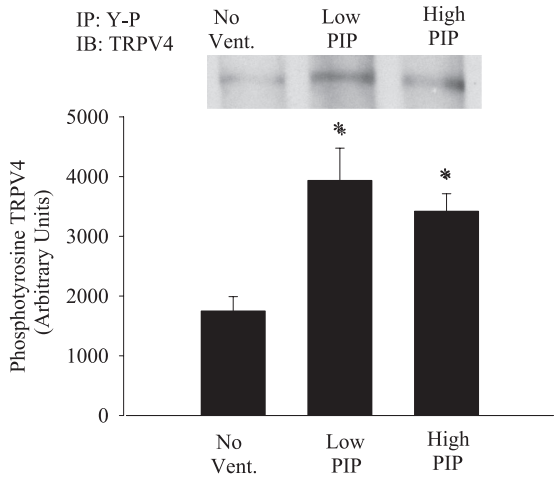

Fig. 5. Tyrosine phosphorylation of TRPV4 in unventilated lungs and isolated perfused lungs exposed to the low PIP and high PIP protocols. Mean values represent phosphorylated TRPV4 obtained from 3 separate lungs in each of the groups. IP, immunoprecipitation; IB, immunoblot; Y-P, phosphotyrosine. *$P < 0.05$ vs. no ventilation (vent.) group.

observed in only 0.3% of the alveolar space in TRPV4$^{-/-}$ mice after 150 min of low PIP ventilation but filled 4.5% of the alveolar space in wild-type mice after the low PIP/30°C protocol. After high PIP ventilation at 40°C, perivascular cuff volume (2.6-fold) and alveolar flooding (2.1-fold) were significantly increased in wild-type mouse lungs compared with those of TRPV4$^{-/-}$ mice. In TRPV4$^{-/-}$ mouse lungs, high PIP ventilation protocols did not affect the Vc/Vw but significantly increased the Vaf/Vas, although these were significantly lower than values obtained in wild-type mice.

DISCUSSION

VILI is a complex syndrome induced by the cellular response to mechanical stress. The syndrome includes a rapid increase in vascular permeability followed by cytokine release and inflammatory cell infiltrates (7, 8, 27). The rapid onset of the increase in vascular permeability compared with the slower increase in cytokine levels and mobilization of inflammatory cell infiltrates some hours later suggest a rapid intracellular signaling cascade of events (33, 47). We evaluated the endothelial permeability increases induced by low or high PIP ventilation and heat using gravimetric K_f, a rapidly responding and repeatable indicator of transvascular fluid filtration and endothelial hydraulic conductivity in the fully recruited lung (26, 31). An increase in endothelial intracellular calcium is a necessary event in the increased permeability induced by numerous receptor ligand-mediated signaling responses (18, 19, 38). We have previously demonstrated that the increase in vascular permeability due to lung overdistention was blocked by gadolinium, an inhibitor of stretch-activated cation channels (28). However, the molecular identity of these channels has not been reported previously. In the present study, we observed that the Ca^{2+}-permeable cation channel TRPV4 is a likely candidate for this stretch-activated cation channel (30). Calcium entry through TRPV4 was an early determinant of the acute permeability increase in lungs following high PIP ventilation, and TRPV4 was activated by arachidonic acid metabolites and EETs to produce the pulmonary vascular permeability increase in the isolated lungs during mechanical stress. Lung inflation caused Ca^{2+} increases via TRPV4, which correlated with the K_f increases. Both the Ca^{2+} increase and K_f increase were blocked by TRPV4$^{-/-}$ deletion, a TRPV channel inhibitor and inhibitors of arachidonic acid metabolism. The K_f increase induced by high pressure ventilation and heat in TRPV4$^{+/+}$ mice was markedly reduced in TRPV4$^{-/-}$ mice at all ventilation times, ventilation pressures, and temperatures for K_f measurement. Therefore, we propose that TRPV4 is the stretch-activated cation channel that initiates lung injury during high volume and pressure ventilation.

The TRPV channels have six transmembrane-spanning segments with a pore loop between segments 5 and 6. These are cation channels with a greater permeability to calcium than sodium (23). TRPV1-4 have promiscuous gating characteristics and respond to temperature, mechanical stimuli, arachidonic acid metabolites, and other chemical stimuli. TRPV2 and -4 mRNA was expressed in mouse lung (13), and TRPV4 is present in mouse lung endothelial and epithelial cells and macrophages (3). Peak gating of TRPV4 with mechanical stretch occurred at the core body temperature of the respective animals, with little response at room temperature (15). Hypotonic solutions activated TRPV4 by phospholipase A2-mediated formation of arachidonic acid products via the cytochrome *P*-450 epoxygenase pathway (40). We have previously implicated calcium entry through stretch-activated cation channels and phospholipase A_2 (PLA2) products in initiating the acute

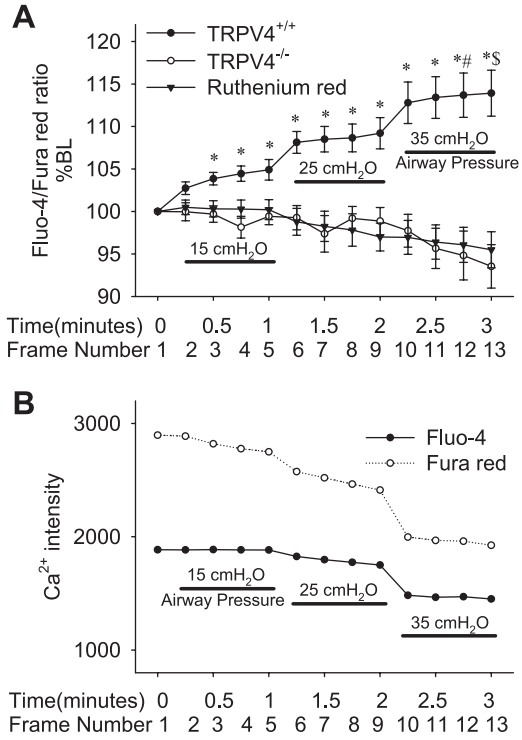

Fig. 6. *A*: mean fluo-4/fura red fluorescence intensity ratios in lungs of TRPV4$^{+/+}$, TRPV4$^{-/-}$, and ruthenium red-treated mice during stepwise increases in constant pressure inflation of the lungs. *B*: representative recordings of the single fluorescence intensity curves obtained for fluo-4 and fura red during airway pressure increases. Images were obtained every 15 s, and the intensity ratios of fluo-4 and fura red were normalized to %baseline (BL). *$P < 0.05$ vs. TRPV4$^{-/-}$ and ruthenium red group in same time. #$P < 0.05$ vs. frames 1–8 in same group. \$$P < 0.05$ vs. frames 1–9 in same group.

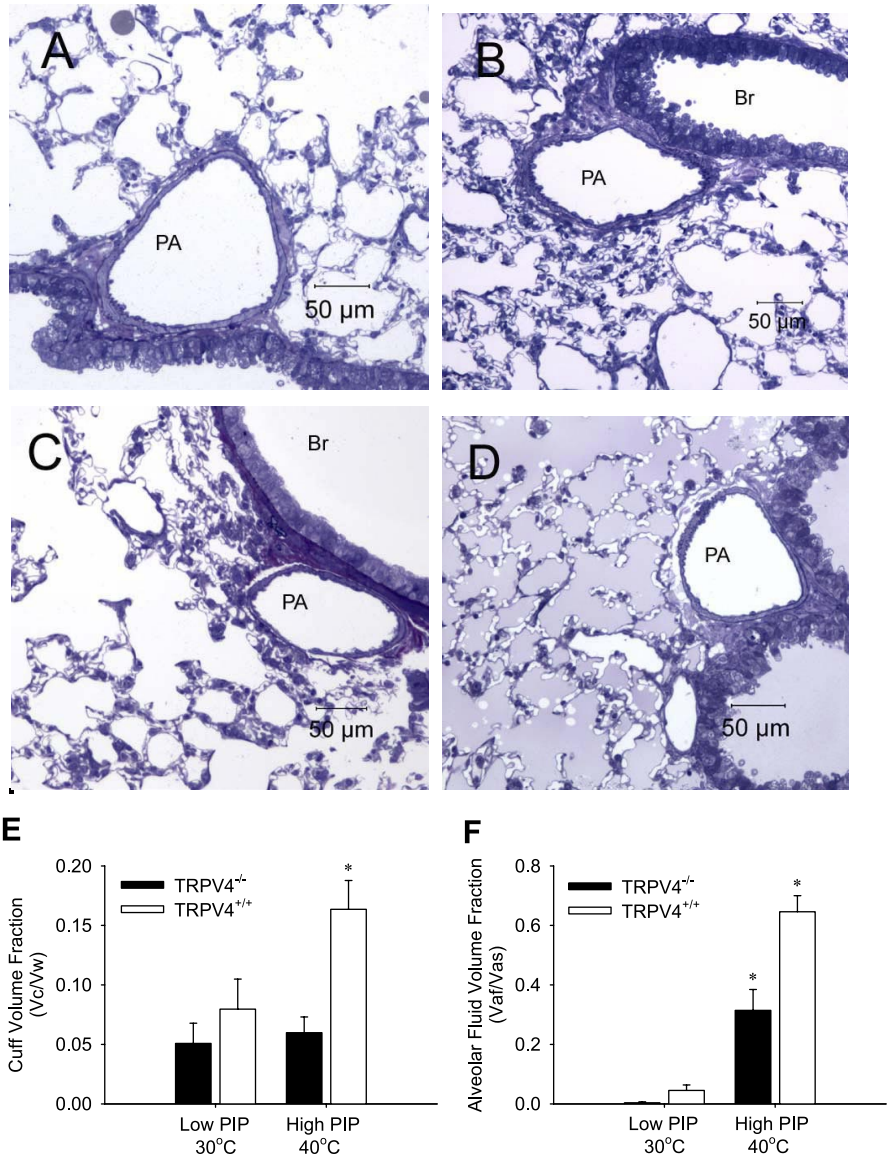

Fig. 7. Microscopic assessment of fluid distribution in perivascular cuffs and alveoli. Representative micrographs of lungs from low PIP/30°C group (*A*, *C*) or high PIP/40°C group (*B*, *D*) in TRPV4$^{-/-}$ (*A*, *B*) or wild-type mice (*C*, *D*). Mean values for cuff volume (V_c) fraction of total wall volume (V_c/V_w; *E*) and alveolar fluid volume (V_{af}) fraction in the alveolar space (V_{af}/V_{as}; *F*) obtained using a point-counting strategy. *$P < 0.05$ vs. all other groups. PA, pulmonary artery; Br, bronchus.

pulmonary vascular permeability increase in response to high PIP ventilation. Parker et al. (28) observed that gadolinium chloride, an effective inhibitor of stretch-activated cation channels, totally blocked the K_f increase induced by high PIP ventilation in isolated perfused rat lungs. Yoshikawa et al. (48) showed that mice deficient in Clara cell secretory protein (CCSP), a modulator of cytosolic PLA2 (cPLA2) activity, had an increased susceptibility to acute VILI, whereas inhibition of PLA_2 attenuated lung vascular permeability increases and edema in both CCSP$^{-/-}$ and wild-type mice after 2 and 4 h of high PIP ventilation. EETs are arachidonic acid metabolites produced by cytochrome *P*-450 epoxygenases that possess important vasodilating and anti-inflammatory properties (9). Arachidonic acid is derived from membrane phospholipids by activation of cytosolic or secreted PLA2. Alternatively, arachidonic acid may be derived from hydrolysis of endocannnabinoids, such as anandamide (arachidonylethanolamide), and by fatty acid amidohydrolases (39). Watanabe et al. (45) demonstrated that the endocannabinoid anandamide and its metabolite, arachidonic acid, activate TRPV4 via the cytochrome *P*-450 epoxygenase-dependent formation of EETs. The same group also showed that mechanical activation of TRPV4 by hypotonic cell swelling depended on the formation of arachidonic acid mediated by PLA2, whereas 4α-PDD and heat activated TRPV4 in a PLA2- and arachidonic acid-independent manner (44). They also suggested that heat activation of TRPV4 depends on the presence of a yet-unknown endogenous ligand, because a heating stimulus failed to activate TRPV4 channels in inside-out patches of human embryonic kidney (HEK293) cells, even though the patches responded to 4α-PDD (21). In the present study, inhibition of TRPV4 (ruthenium red), *P*-450 epoxygenase (miconazole), or arachidonic acid (methanandamide) attenuated the endothelial permeability increase induced by both high PIP ventilation and heat. These results suggest that TRPV4 activation via arachidonic acid and EETs is a major contributor to acute VILI.

More recent findings have demonstrated a relationship of tyrosine phosphorylation to TRP channel activation. Mutations at positions Tyr^{555} in transmembrane segment-3 (TM3) inhibited channel activation by 4α-PDD and heat (42), whereas Xu

et al. (46) also implicated tyrosine phosphorylation of TRPV4 at Tyr^{253} as essential for the response to hypotonic stress and proposed involvement of Src family tyrosine kinases in this response. In a previous study in isolated rat lungs, global tyrosine kinase inhibition with genistein attenuated the K_f increase following high PIP ventilation (29). More recently, Miyahara et al. (20) attenuated high PIP-induced increases in K_f using a Src family kinase inhibitor. In the present study, we show an increased tyrosine phosphorylation of the TRPV4 protein in both ventilation groups compared with unventilated lungs, but specific phosphorylation sites were not identified. Characterization of specific TRPV4 activation sites in different cell types will be required to fully understand the various gating paradigms.

TRPV4-mediated Ca^{2+} entry has been implicated in both endothelial cells and the K_f response in intact lungs. Vriens et al. (40) reported that the $[Ca^{2+}]_i$ responses to arachidonic acid, cell swelling, and heat for $TRPV4^{-/-}$ mouse aortic endothelial cells were significantly less than those for the same cells from $TRPV4^{+/+}$ mice. They proposed that the residual Ca^{2+} response to arachidonic acid or downstream metabolites of arachidonic acid was due to activation of Ca^{2+}-permeable channels other than TRPV4, or to possible upregulation of other thermosensitive or osmosensitive channels. Alvarez et al. (3) showed that both 5,6-EET and 14,15-EET increased K_f with physiological perfusate but evoked a small increase in permeability in isolated rat lungs, even with 0.02 mmol/l Ca^{2+} in the buffer. These results suggest that other pathways or channels in addition to TRPV4 may be activated by arachidonic acid via EETs and may augment Ca^{2+} entry during the endothelial permeability increases. Microscopic assessment revealed that TRPV4 preferentially targeted the alveolar septal microvessels and typically caused endothelial blebs or breaks, whereas store-operated TRP channels targeted extra-alveolar vessels and caused formation of gaps at endothelial cell junctions. Disruption of the septal barrier is more likely to promote alveolar flooding and impair gas exchange than disruption in extra-alveolar vessels (3). In the present study, $TRPV4^{-/-}$ and $TRPV4^{+/+}$ had approximately equal cuff volumes of edema and negligible alveolar flooding during low pressure/low temperature ventilation, but $TRPV4^{+/+}$ lungs had edema cuff volumes that were 2.6 times, and alveolar flooding 2.1 times, that measured in $TRPV4^{-/-}$ lungs after high PIP/high temperature ventilation. It is apparent that the edema due to mechanical strain on both alveolar and extra-alveolar endothelium was greatly attenuated by the absence of TRPV4 channels. Mechanical effects of interdependence and the low perivascular interstitial pressures generated by high lung volumes would be expected to generate high transmural filtration pressures in the extra-alveolar vessels (35). To the extent that this regional edema reflects local filtration, these studies suggest that TRPV4 plays critical role in mechanical stress-induced endothelial permeability in both alveolar and extra-alveolar vessels.

Yoshikawa et al. (49) previously reported that VILI was related to both ventilation time and airway pressure. Many investigators have demonstrated that high PIP ventilation increases total lung K_f (20), segmental lung K_f (32), bacterial translocation from the lung into the systemic circulation (25), bronchoalveolar lavage albumin concentration (8), W/D ratio, inflammatory cytokines (5, 37), and lung myeloperoxidase (48). Our present study also implicates temperature acting through TRPV4 as a modulator of mechanical injury in the lung (Fig. 1). Akinci et al. (1) reported that systemic chemokine and cytokine levels were significantly elevated by heating to 41°C of body temperature with 30 cmH_2O PIP ventilation for 1 h in rat. In contrast, hypothermia during injurious ventilation prevented vascular and epithelial injury and preserved lung mechanics in rats (16). The present investigation of different temperature effects on K_f measurements indicated a greater increase in endothelial permeability at 40 than 35°C but little difference between responses at 30 and 35°C. This suggests a temperature threshold for isolated perfused mouse lungs of C57BL/6 male mice >35°C. Moreover, K_f was significantly increased by high PIP ventilation compared with low PIP at both temperatures. Guler et al. (11) showed that TRPV4 channels mediated heat-evoked currents at temperatures >27°C in *Xenopus* oocytes, but that the threshold for TRPV4 activation was ~34°C in the HEK293 cells (11). Although the temperatures entering the lungs were accurately controlled, a small temperature drop across the lung of 2.5 ± 0.1°C in the 35°C group and 3.3 ± 0.1°C in the 40°C group was observed, suggesting that the entire lung may not have experienced exactly the same perfusate temperature. In any case, our data suggest that a fever within a clinically relevant range could sensitize the TRPV4 channel to mechanical gating and augment lung injury due to mechanical ventilation.

To further confirm the role of calcium entry through TRPV4 channels, we measured intravascular calcium concentrations in alveolar vessels using fluorescence microscopy and calcium-sensitive dyes. Previous studies using cultured cells demonstrated that endothelial cell membrane stretch induced by hypotonic cell swelling or shear stress induced by solution flow across endothelial monolayers increased intracellular Ca^{2+} within a physiological range of temperatures (10, 23). Furthermore, a high vascular pressure increased the mean endothelial $[Ca^{2+}]_i$ and amplified $[Ca^{2+}]_i$ oscillations in constant pressure inflated, perfused rat lungs in a $GdCl_3$-sensitive manner (12). However, the Ca^{2+} increase induced by lung inflation with high airway pressures in ex vivo isolated perfused lungs has not been demonstrated previously. We used two Ca^{2+} indicator dyes, fluo-4 AM and fura red AM, for ratiometric imaging because increased intracellular calcium causes the fluorescent intensity of fluo-4 to increase but the intensity of fura red to decrease (24). Ratiometric analysis eliminates artifactual fluorescence changes during attenuation of the fluorescent signal by a reduction in endothelial cell volumes due to stretch of the alveolar capillaries and arterioles during lung inflation (Fig. 7*B*) (17). Our finding that the $[Ca^{2+}]_i$ elevation in inflated lungs of $TRPV4^{+/+}$ mice was eliminated in $TRPV4^{-/-}$ or ruthenium red-treated mice strongly suggests that lung inflation and alveolar distention provoked Ca^{2+} entry through TRPV4 channels.

In summary, we have demonstrated that the acute increase in vascular permeability in VILI is strongly associated with Ca^{2+} entry via TRPV4 evoked by both high pressure ventilation and heat. Therefore, TRPV4 and its transduction pathways may be important therapeutic targets for prevention of VILI.

GRANTS

This research was supported by National Institutes of Health Grants P01-HL-66299 and K08-MH-64702 and a grant from the American Heart Association.

REFERENCES

1. **Akinci OI, Celik M, Mutlu GM, Martino JM, Tugrul S, Ozcan PE, Yilmazbayhan D, Yeldandi AV, Turkoz KH, Kiran B, Telci L, Cakar N.** Effects of body temperature on ventilator-induced lung injury. *J Crit Care* 20: 66–73, 2005.
2. **Alvarez DF, King JA, Townsley MI.** Resistance to store depletion-induced endothelial injury in rat lung after chronic heart failure. *Am J Respir Crit Care Med* 172: 1153–1160, 2005.
3. **Alvarez DF, King JA, Weber D, Addison E, Liedtke W, Townsley MI.** Transient receptor potential vanilloid 4-mediated disruption of the alveolar septal barrier: a novel mechanism of acute lung injury. *Circ Res* 99: 988–995, 2006.
4. **Bates DO, Harper SJ.** Regulation of vascular permeability by vascular endothelial growth factors. *Vasc Pharmacol* 39: 225–237, 2002.
5. **Belperio JA, Keane MP, Lynch JP, Strieter RM.** The role of cytokines during the pathogenesis of ventilator-associated and ventilator-induced lung injury. *Semin Respir Crit Care Med* 27: 350–364, 2006.
6. **Brower RG, Matthay MA, Morris A, Schoenfeld D, Thompson BT.** Ventilation with lower tidal volumes as compared with traditional tidal volumes for acute lung injury and respiratory distress syndrome. *N Engl J Med* 342: 1301–1308, 2000.
7. **Dos Santos CC, Slutsky AS.** Invited review: mechanisms of ventilator-induced lung injury: a perspective. [comment]. *J Appl Physiol* 89: 1645–1655, 2000.
8. **Dreyfuss D, Saumon G.** Ventilator induced lung injury: lessons from experimental studies. *Am J Respir Crit Care Med* 157: 294–323, 1998.
9. **Fang X, Kaduce TL, Weintraub NL, Harmon S, Teesch LM, Morisseau C, Thompson DA, Hammock BD, Spector AA.** Pathways of epoxyeicosatrienoic acid metabolism in endothelial cells. Implications for the vascular effects of soluble epoxide hydrolase inhibition. *J Biol Chem* 276: 14867–14874, 2001.
10. **Gao X, Wu L, O'Neil RG.** Temperature-modulated diversity of TRPV4 channel gating: activation by physical stresses and phorbol ester derivatives through protein kinase C-dependent and -independent pathways. *J Biol Chem* 278: 27129–27137, 2003.
11. **Guler A.** Heat-evoked activation of the ion channel, TRPV4. *J Neurosci* 22: 6408–6414, 2002.
12. **Kuebler WM, Ying X, Bhattacharya J.** Pressure-induced endothelial Ca(2+) oscillations in lung capillaries. *Am J Physiol Lung Cell Mol Physiol* 282: L917–L923, 2002.
13. **Kunert-Keil C, Bisping F, Kruger J, Brinkmeier H.** Tissue-specific expression of TRP channel genes in the mouse and its variation in three different mouse strains. *BMC Genomics* 7: 159, 2006.
14. **Liedtke W.** Vanilloid receptor-related osmotically activated channel (VR-OAC), a candidate vertebrate osmoreceptor. *Cell* 103: 525–535, 2000.
15. **Liedtke W.** TRPV channels' function in osmo- and mechanotransduction. In: *TRP Ion Channel Function in Sensory Transduction and Cellular Signaling Cascades*, edited by Liedtke W and Heller S. Boca Raton, FL: CRC/Taylor & Francis, 2006, p. 303–318.
16. **Lim CM, Hong SB, Koh Y, Lee SD, Kim WS, Kim DS, Kim WD.** Hypothermia attenuates vascular manifestations of ventilator-induced lung injury in rats. *Lung* 181: 23–34, 2003.
17. **Marie I, Beny JL.** Calcium imaging of murine thoracic aorta endothelium by confocal microscopy reveals inhomogeneous distribution of endothelial cells responding to vasodilator agents. *J Vasc Res* 39: 260–267, 2002.
18. **Mehta D, Malik AB.** Signaling mechanisms regulating endothelial permeability. *Physiol Rev* 86: 279–367, 2006.
19. **Michel CC, Curry FE.** Microvascular permeability. *Physiol Rev* 79: 703–761, 1999.
20. **Miyahara T, Weber DS, Drake DA, Anghelescu M, Parker JC.** Phosphatidylinositol-3 kinase, Src, and Akt modulate acute ventilation-induced permeability increases in mouse lungs. *Am J Physiol Lung Cell Mol Physiol* 293: L11–L21, 2007.
21. **Nilius B, Watanabe H, Vriens J.** The TRPV4 channel: structure-function relationship and promiscuous gating behaviour. *Pflügers Arch* 446: 298–303, 2003.
22. **Nilius B, Vriens J, Prenen J, Droogmans G, Voets T.** TRPV4 calcium entry channel: a paradigm for gating diversity. *Am J Physiol Cell Physiol* 286: C195–C205, 2004.
23. **O'Neil RG, Heller S.** The mechanosensitive nature of TRPV channels. *Pflügers Arch* 451: 193–203, 2005.
24. **Oishi H, Budel S, Schuster A, Stergiopulos N, Meister JJ, Beny JL.** Cytosolic-free calcium in smooth-muscle and endothelial cells in an intact arterial wall from rat mesenteric artery in vitro. *Cell Calcium* 30: 261–267, 2001.
25. **Ozcan P, Cakar N, Tugrul S, Akinci O, Cagatay A, Yilmazbayhan D, Esen F, Telci L, Akpir K.** The effects of airway pressure and inspiratory time on bacterial translocation. *Anesth Analg* 104: 391–396, 2007.
26. **Parker JC, Gillespie MN, Taylor AE, Martin SL.** Capillary filtration coefficient, vascular resistance and compliance in isolated mouse lungs. *J Appl Physiol* 87: 1421–1427, 1999.
27. **Parker JC, Hernandez LA, Peevy K.** Mechanisms of ventilator induced injury. *Crit Care Med* 21: 131–143, 1993.
28. **Parker JC, Ivey C, Tucker A.** Gadolinium prevents high airway pressure induced permeability increases in isolated rat lungs. *J Appl Physiol* 84: 1113–1118, 1998.
29. **Parker JC, Ivey CL, Tucker A.** Phosphotyrosine phosphatase and tyrosine inhibition modulate airway pressure induced lung injury. *J Appl Physiol* 85: 1753–1761, 1998.
30. **Parker JC, Miyahara T, Anghelescu M.** Acute passive and active changes in microvascular permeability during lung distention. In: *Ventilator Induced Lung Injury*, edited by Dreyfuss D, Saumon G, and Hubmayr RD. New York: Taylor & Francis, 2006, p. 69–95.
31. **Parker JC, Townsley MI.** Evaluation of lung injury in rats and mice. *Am J Physiol Lung Cell Mol Physiol* 286: L231–L246, 2004.
32. **Parker JC, Yoshikawa S.** Vascular segmental permeabilities at high peak inflation pressure in isolated rat lungs. *Am J Physiol Lung Cell Mol Physiol* 283: L1203–L1209, 2002.
33. **Quinn DA, Moufarrej RK, Volokhov A, Hales CA.** Interactions of lung stretch, hyperoxia, and MIP-2 production in ventilator-induced lung injury. *J Appl Physiol* 93: 517–525, 2002.
34. **Song C, Al Mehdi AB, Fisher AB.** An immediate endothelial cell signaling response to lung ischemia. *Am J Physiol Lung Cell Mol Physiol* 281: L993–L1000, 2001.
35. **Taylor AE, Parker JC.** The interstitial spaces and lymph flow. In: *Handbook of Physiology. The Respiratory System. Circulation and Nonrespiratory Functions*. Bethesda, MD: Am Physiol Soc, 1986, sect. 3, vol. I, p. 167–320.
36. **Tiruppathi C, Minshall RD, Paria BC, Vogel SM, Malik AB.** Role of Ca(2+) signaling in the regulation of endothelial permeability. *Vasc Pharmacol* 39: 173–185, 2002.
37. **Uhlig S, Uhlig U.** Pharmacological interventions in ventilator-induced lung injury. *Trends Pharmacol Sci* 25: 592–600, 2004.
38. **Usatyuk PV, Fomin VP, Shi S, Garcia JGN, Schaphorst K, Natarajan V.** Role of Ca(2+) in diperoxovanadate-induced cytoskeletal remodeling and endothelial cell barrier function. *Am J Physiol Lung Cell Mol Physiol* 285: L1006–L1017, 2003.
39. **Vriens J, Owsianik G, Fisslthaler B, Suzuki M, Janssens A, Voets T, Morisseau C, Hammock BD, Fleming I, Busse R, Nilius B.** Modulation of the Ca(2+) permeable cation channel TRPV4 by cytochrome P450 epoxygenases in vascular endothelium. *Circ Res* 97: 908–915, 2005.
40. **Vriens J, Watanabe H, Janssens A, Droogmans G, Voets T, Nilius B.** Cell swelling, heat, and chemical agonists use distinct pathways for the activation of the cation channel TRPV4. *Proc Natl Acad Sci USA* 101: 396–401, 2006.
41. **Ware LB, Matthay MA.** The acute respiratory distress syndrome. [comment]. *N Engl J Med* 342: 1334–1349, 2000.
42. **Watanabe H.** Activation of TRPV4 channels (hVRL-2/mTRP12) by phorbol derivatives. *J Biol Chem* 277: 13569–13577, 2002.
43. **Watanabe H.** Heat-evoked activation of TRPV4 channels in an HEK293 cell expression system and in native mouse aorta endothelial cells. *J Biol Chem* 277: 47044–47051, 2002.
44. **Watanabe H, Vriens J, Prenen J, Droogmans G, Voets T, Nilius B.** Anandamide and arachidonic acid use epoxyeicosatrienoic acids to activate TRPV4 channels. *Nature* 424: 434–438, 2003.
45. **Wurfel MM.** Microarray-based analysis of ventilator-induced lung injury. *Proc Am Thorac Soc* 4: 77–84, 2007.
46. **Xu H, Zhao H, Tian W, Yoshida K, Roullet JB, Cohen DM.** Regulation of a transient receptor potential (TRP) channel by tyrosine phosphorylation. SRC family kinase-dependent tyrosine phosphorylation of TRPV4 on TYR-253 mediates its response to hypotonic stress. *J Biol Chem* 278: 11520–11527, 1928.

47. **Yoshikawa S, King JA, Lausch RN, Penton AM, Eyal FG, Parker JC.** Acute ventilator-induced vascular permeability and cytokine responses in isolated and in situ mouse lungs. *J Appl Physiol* 97: 2190–2199, 2004.
48. **Yoshikawa S, Miyahara T, Reynolds SD, Stripp BR, Anghelescu M, Eyal FG, Parker JC.** Clara cell secretory protein and phospholipase A2 activity modulate acute ventilator-induced lung injury in mice. *J Appl Physiol* 98: 1264–1271, 2005.
49. **Yoshikawa S, King JA, Reynolds SD, Stripp BR, Parker JC.** Time and pressure dependence of transvascular Clara cell protein, albumin, and IgG transport during ventilator-induced lung injury in mice. *Am J Physiol Lung Cell Mol Physiol* 286: L604–L612, 2004.